INTERNATIONAL JOURNAL OF OPTIMIZATION IN CIVIL ENGINEERING
Int. J. Optim. Civil Eng., 2018; 8(1):77-99

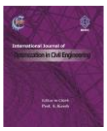

DAMAGE AND PLASTICITY CONSTANTS OF CONVENTIONAL AND HIGH-STRENGTH CONCRETE PART I: STATISTICAL OPTIMIZATION USING GENETIC ALGORITHM

M. Moradi[1], A. R. Bagherieh[1*, †] and M. R. Esfahani[2]
[1]*Department of Civil Engineering, Malayer University, Malayer, Iran*
[2]*Department of Civil Engineering, Ferdowsi University of Mashhad, Mashhad, Iran*

ABSTRACT

The constitutive relationships presented for concrete modeling are often associated with unknown material constants. These constants are in fact the connectors of mathematical models to experimental results. Experimental determination of these constants is always associated with some difficulties. Their values are usually determined through trial and error procedure, with regard to experimental results. In this study, in order to determine the material constants of an elastic-damage-plastic model proposed for concrete, the results of 44 uniaxial compression and tension experiments collected from literature were used. These constants were determined by investigating the consistency of experimental and modeling results using a genetic algorithm optimization tool for all the samples; then, the precision of resulted constants were investigated by simulating cyclic and biaxial loading experiments. The simulation results were compared to those of the corresponding experimental data. The results observed in comparisons indicated the accuracy of obtained material constants in concrete modeling.

Keywords: Reinforced concrete; genetic algorithm; constitutive modeling; damage; plasticity.

Received: 2 March 2017; Accepted: 20 June 2017

1. INTRODUCTION

Concrete is the most used construction material [1]. Conventional concrete is a composite material consisting of cement, water, sand, and aggregates. Despite negative effects of this composite structure, concrete is still known as an essential material [2]. In general, and particularly with regard to concrete, inefficient modeling of engineering materials is one of

[*]Corresponding author: Department of Civil Engineering, Malayer University
[†]E-mail address: bagheri@malayeru.ac.ir (A. R. Bagherieh)

the factors resulting in weakness of structural analysis [3]. Concrete structures are usually analyzed using finite element method. The analysis of structural engineering problems using finite element method always includes primary-boundary conditions and the material response to these conditions. The establishment of a relationship between these two factors requires a constitutive model [4]. Constitutive rules are generally determined based on a set of experiments [5-6]. Experimental studies on concrete through uniaxial and multi-axial tests associated with compressive, tensile, and cyclic loading showed that the concrete response included strain-softening/hardening behavior, degradation of stiffness, volume dilation, anisotropy, and irreversible deformations.

In recent years, several constitutive models have been proposed for concrete. These models are usually classified into five categories including the models derived from empirical relationships, elasticity models, plasticity models, models based on continuous damage theory, and micromechanics models [7]. Determining the constitutive relationships directly and empirically through tests seems to be an appropriate way, taken into account even in recent years [8-11]. In spite of using artificial intelligence such as fuzzy algorithms in this field [8-9], these studies have often used multi-variable regression [10-11]. Despite their high accuracy and simplicity, these relationships can only simulate a specific behavior or a specific loading state; further, it is not possible to use them for general modeling of concrete as finite element method. Linear elastic models are the simplest constitutive models available in the literature [5]. In elastic models, the concrete behaves in a linear elastic manner until reaching the ultimate stress and the subsequent rupture in brittle state; however, these constitutive models are usually inappropriate for concrete, because concrete is considered as a pressure-sensitive material, which generally has a strictly non-linear and non-elastic performance under the applied load [12]. Plasticity models have an appropriate agreement with single and multi-axial compressive behavior of the concrete. Irreversible deformations and volume expansion can be expressed using the elasticity theory {Fig. 1(a)}, but macroscopic spread of the micro-cracks leads to degradation of the initial stiffness and reduction of the material effective cross-section. Expression of this phenomenon based on classic plasticity is very complicated [14], while it can be simply defined using the damage theory {Fig. 1(b)}. As shown in Fig. 1, the damage and plasticity theories are combined with each other to achieve an appropriate model according to the real behavior of the concrete [14-15]. One of the simplest and most practical methods for combining these two theories is using the effective stress space [14-15]. In this method, it is assumed that the materials have no cracks and discontinuities and are modeled elastoplastically in the effective stress space; then, the degradation of stiffness and reduction of the effective cross-section caused by micro-cracks are applied on the results of effective stress space using damage theory, so that actual results are achieved.

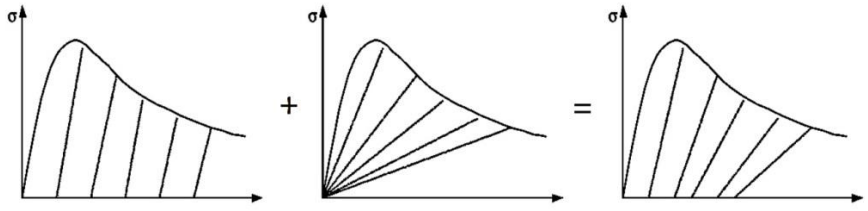

(a) plastic behavior (b) damage behavior (c) plastic-damage

Figure 1. Typical uniaxial compressive stress-strain diagram of concrete [13]

Several researchers have used the effective stress space method to combine the isotropic or anisotropic damage with the plasticity theory [14-20]. These studies have generally focused on demonstrating the models ability to describe all the behavioral characteristics of concrete. One of problems of the relationships of damage-plasticity models is the set of constants which should be determined beforehand. These constants are in fact the connectors of the mathematical models to the experimental results, whose improper determination leads to the model failure in predicting the results; accordingly, these constants are essential in models. Experimental determination of these constants is usually associated with problems. Generally, inverse methods are used for determination of these values in order to prove the efficiency of models presented in the literature [13-21]; in other words, after identifying the modeling relationships through trial and error, the values of constitutive relationship constants are determined with regard to the experimental results. The models presented in these studies are often validated based on a very limited number of experimental results and, in most cases, it is impossible to make any primary estimation of the constants. Several studies have expressed that it is possible to obtain appropriate values for modeling constants by matching the modeling through trial and error with uniaxial compressive and tensile diagrams [13, 17-19]; Wardeh and Toutanji [22] used the genetic algorithm optimization method to determine the numeric constants of an elastic-damage model. Although their results were promising, this modeling method is unable to describe the irreversible deformations of concrete.

In this study, the elastic-plastic-damage model of Voyiadjis and Taqieddin [18], which had simple modeling relationships, was selected and implemented in MATLAB. Then, based on a set of experimental results, the optimal values of the damage and plasticity constants were determined using the genetic algorithm tool of this software. In the next sections, the elastic-plastic-damage model formulated by Voyiadjis and Taqieddin [18] will be explored.

2. ELASTIC-PLASTIC-DAMAGE MODEL OF VOYIADJIS & TAQIEDDIN [18]

In Voyiadjis and Taqieddin's model [18], the effective stress method has been used for developing the relationships. Based on this method, the elastoplastic response of the problem is calculated regardless of the effect of damage on the effective stress space, and then the damage effect is applied to this response. This model includes a criterion of plastic yielding presented in the effective stress space [14-21]; further, the damage criterion used in this model has been obtained based on the results of Tao and Phillips [13]. This damage criterion is isotropic and includes two numeric variables of damage for compression and tension. The model of Voyiadjis and Taqieddin [18] will be described in following sections; furthermore, necessary modifications for this model will be proposed.

Eq. (1) presents the effective stress tensor (stress in undamaged configuration) based on Hooke's Law.

$$\bar{\sigma}_{ij} = \bar{E}_{ijkl}(\varepsilon_{kl} - \varepsilon_{kl}^{p}) \quad (1)$$

In this equation, ε_{kl} and ε_{kl}^{p} indicate overall and plastic strain tensors, respectively. $\bar{E}_{ijkl}$ stands for the fourth-order tensor of the undamaged isotropic elasticity and is calculated through Eq. (2). In Eq. (2), δ_{ij} indicates Kronecker delta tensor. $\bar{G}$ and $\bar{K}$, respectively, indicate the shear modulus and bulk modulus of the undamaged materials. These constants can be expressed based on the elasticity modulus (E) and Poisson's ratio (ν) of the undamaged materials {Eq. (2)}.

$$\bar{E}_{ijkl} = 2\bar{G}(\frac{1}{2}(\delta_{ik}\delta_{jl} + \delta_{il}\delta_{jk}) - \frac{1}{3}\delta_{ij}\delta_{kl}) + \bar{K}\delta_{ij}\delta_{kl}; \bar{K} = \frac{E}{3(1-2\nu)}; \bar{G} = \frac{E}{2(1+\nu)} \quad (2)$$

Configuration of the materials in the damaged state can be presented similarly to the Eq. (1) {Eq. (3)}.

$$\sigma_{ij} = E_{ijkl}(\Phi)(\varepsilon_{kl} - \varepsilon_{kl}^{p}) \quad (3)$$

E_{ijkl} is the fourth-order tensor of elasticity in the damaged configuration. In the damage model of Tao and Phillips [13], the stress-strain relation contains a numeric variable of isotropic damage (Φ). Accordingly, E_{ijkl} is defined as follows:

$$E_{ijkl} = (1 - \Phi)\bar{E}_{ijkl} \quad (4)$$

By inserting Eq. (4) in Eq. (3) and considering Eq. (1), the relation of the real stress tensor is obtained {Eq. (5)} [18].

$$\sigma_{ij} = (1 - \Phi)\bar{\sigma}_{ij} \quad (5)$$

The numeric variable of Φ represents the macroscopic effect of the materials damage mechanism. This variable is obtained from the weighted average of the variables of compressive damage (φ^{-}) and tensile damage (φ^{+}). The ratio of the coefficients of compressive and tensile damage variables is considered equal to the ratio of the numerical contraction of the compressive and tensile stress tensor to the numerical contraction of overall stress, respectively [13] {Eq. (6)}. Numerical contraction of the second order tensor is expressed as $[\![X_{ij}]\!] = X_{ij}X_{ij}$.

$$\Phi = \frac{[\![\bar{\sigma}_{ij}^{+}]\!]\varphi^{+} + [\![\bar{\sigma}_{ij}^{-}]\!]\varphi^{-}}{[\![\bar{\sigma}_{ij}]\!]} \quad (6)$$

According to the above equation, in order to consider the effect of damage mechanism on the nonlinear performance of concrete under tension and pressure, the effective stress tensor is decomposed into two compressive ($\bar{\sigma}_{ij}^{-}$) and tensile ($\bar{\sigma}_{ij}^{+}$) parts {Eq. (7)}. This is done using spectral decomposition {Eq. (8)} [14, 16]. The value of

P_{ijpq}^{+} is presented in Eq. (9).

$$\bar{\sigma}_{ij} = \bar{\sigma}_{ij}^{+} + \bar{\sigma}_{ij}^{-} \tag{7}$$

$$\bar{\sigma}_{ij}^{+} = P_{ijpq}^{+}\bar{\sigma}_{ij} \tag{8}$$

$$P_{ijpq}^{+} = \sum_{k=1}^{3} H(\hat{\bar{\sigma}}^{(k)}) n_i^{(k)} n_j^{(k)} n_p^{(k)} n_q^{(k)} \tag{9}$$

$\hat{\bar{\sigma}}^{(k)}$ and $n_i^{(k)}$ indicate the values of the effective stress tensor and its main equivalent directions. The negative part of the stress tensor can be easily calculated based on Eq. 7 {Eq. (10)}.

$$\bar{\sigma}_{ij}^{-} = \bar{\sigma}_{ij} - \bar{\sigma}_{ij}^{+} \tag{10}$$

In order to model the concrete through incremental writing of the above equations, it is enough to determine the values of plastic strain and the numerical variable of damage in each step. The method of determination of these values is briefly explained below (See Voyiadjis and Taqieddin [18] for more details).

2.1 Plasticity yield surface and hardening functions

A vital component in modeling based on the plasticity theory is the yield surface. Eq. (11) shows the yield criterion used in this study [14]. This yield criterion has been successful in simulating the behavior of concrete under uniaxial, biaxial, and multi-axis load and cyclic loading [14-21]. In Eq. (11), this criterion is presented in the effective stress space.

$$f = \sqrt{3\bar{J}_2} + \alpha\bar{I}_1 + \beta H(\hat{\bar{\sigma}}_{max})\hat{\bar{\sigma}}_{max} - (1-\alpha)c^{-}(\kappa^{-}) = 0 \tag{11}$$

In the above equation, $\bar{I}_1 = \bar{\sigma}_{kk}$ and $\bar{J}_2 = \bar{S}_{ij}\bar{S}_{ij}/2$ indicate the first invariable of effective stress tensor $\bar{\sigma}_{ij}$ and the second invariable of effective stress deviator tensor ($\bar{S}_{ij} = \bar{\sigma}_{ij} - \bar{\sigma}_{kk}\delta_{ij}/3$), respectively. H is the Heaviside function. The value of this function is equal to 1 if the maximum principal stress ($\hat{\bar{\sigma}}_{max}$) is greater than 0; otherwise, it is equal to 0. α is a constant number based on uniaxial (f_0^{-}) and biaxial (f_{b0}^{-}) compressive resistance of concrete and is calculated using Eq. (12) [14].

$$\alpha = \frac{\left(f_{b0}^{-}/f_0^{-}\right) - 1}{2\left(f_{b0}^{-}/f_0^{-}\right) - 1} \tag{12}$$

In Eq. (11), $\kappa^{\pm}$ is the equivalent plastic strain in tension and pressure {Eq. (13) and (14)} [16]. These parameters are also known as hardening variables.

$$\kappa^{+} = \int_{0}^{t} \dot{\kappa}^{+} dt \tag{13}$$

$$\kappa^{-} = \int_{0}^{t} \dot{\kappa}^{-} dt \tag{14}$$

$\dot{\kappa}^{+}$ and $\dot{\kappa}^{-}$are the equivalent plastic strain rates under tension and pressure, respectively. Lee and Fenves [14] have proposed Eq. (15) and (16) for calculating them.

$$\dot{\kappa}^{+} = r\hat{\dot{\varepsilon}}^{p}_{max} \tag{15}$$

$$\dot{\kappa}^{-} = -(1-r)\hat{\dot{\varepsilon}}^{p}_{min} \tag{16}$$

In the above equations, r is a numerical coefficient calculated based on the value of main stresses {Eq. (17)} [14]. In certain states, such as uniaxial pressure and tension, the value of this variable is obtained 0 and 1, respectively.

$$r = \frac{\sum_{i=1}^{3}\langle\hat{\bar{\sigma}}_i\rangle}{\sum_{i=1}^{3}|\hat{\bar{\sigma}}_i|} \tag{17}$$

$\hat{\bar{\sigma}}_i$ in Eq. (17) is equivalent to the eigenvalues of the effective stress tensor. In this equation, Macaulay brackets are used to eliminate negative values. This function is defined as $\langle x\rangle = 0.5(|x| + x)$.

The non-associated flow rule has been used in this model [18]. In other words, the yield function and the plastic potential are not matched. The plastic strain rate tensor is calculated by differentiating from the plastic potential function of F^{p} in terms of the effective stresses, and using the parameter $\dot{\lambda}$ of the plastic flow according to Eq. (18).

$$\dot{\varepsilon}^{p}_{ij} = \dot{\lambda}\frac{\partial F^{p}}{\partial \bar{\sigma}_{ij}} \tag{18}$$

Lee and Fenves [14] defined the plastic potential function F^{p} with Drucker Prager structure {Eq. (19)}.

$$F^{p} = \sqrt{3\bar{J}_2} + \alpha^{p}\bar{I}_1 \tag{19}$$

In the above equation, α^{p} is a numerical variable affecting the value of dilation of the model. In the present research, this variable is assumed equal to 0.2 just as in other studies in this field [14, 15, 18].

The variable β in Eq. (11) is the Barcelona model constant whose value has been defined by Lee and Fenves [14] as a dimensionless function based on the compressive and tensile cohesion $c^{\pm}$ {Eq. (20)}.

$$\beta(\kappa^{\pm}) = (1-\alpha)\frac{c^{-}(\kappa^{-})}{c^{+}(\kappa^{+})} - (1+\alpha) \tag{20}$$

Cohesion variables are equivalent to the evolutionary stresses in the effective stress space caused by plastic hardening/softening under the uniaxial tension and pressure. Voyiadjis and Taqieddin [18] have presented the values of these variables based on the equivalent uniaxial strain in accordance with Eq. (21) and (22).

$$c^{-}(\kappa^{-}) = f_0^{-} + Q[1-\exp(-w\kappa^{-})] \tag{21}$$

$$c^{+}(\kappa^{+}) = f_0^{+} + h\kappa^{+} \tag{22}$$

In above equations, f_0^{-} and f_0^{+} indicate, respectively, the compressive and tensile stresses in which the concrete non-linear behavior begins. Further, Q, w, and h are the constants of the materials. Voyiadjis and Taqieddin [14] have determined the values of these constants through trial and error, with regard to the agreement of experimental results and modeling of the diagrams of the concrete uniaxial pressure and tension.

2.2 Calculation of numerical variable of damage

Tao and Phillps [13] have presented a damage surface for controlling the damage occurrence similar to the case of the plastic state {Eq. (23)}. As previously mentioned, the numerical variables of damage in this model were defined for the pressure and tension, thus the damage level function $g^{\pm}$ is also defined for the compressive and tensile states [18]. It should be noted that the model presented by Tao and Phillips [13] was an elastic-damage model in which plasticity effects had not been taken into account.

$$g^{\pm} = Y^{\pm} - Y_0^{\pm} - Z^{\pm} \tag{23}$$

In this equation, $Y^{\pm}$ and $Y_0^{\pm}$ are, respectively, damage conjugate forces and initial conjugate forces of the tensile and compressive damage threshold. Damage initiation is controlled by $Y_0^{\pm}$. In the damage process, the initial damage level changes. This change is defined based on evolutionary rules by $Z^{\pm}$ variables {Eq. (24)} [18].

$$Z^{\pm} = \frac{1}{a^{\pm}}\left(\frac{\varphi^{\pm}}{1-\varphi^{\pm}}\right)^{\frac{1}{b^{\pm}}} \tag{24}$$

In the above equation, $a^{\pm}$ and $b^{\pm}$ are four constants of the materials and are determined through trial and error based on concrete testing under uniaxial pressure and tension [13, 18-20].

To calculate the values of the damage conjugate forces ($Y^{\pm}$), Tao and Phillps [13] used Eq. (25) and (26).

$$Y^{+}=\frac{1}{2}\frac{[\![\sigma_{ij}^{+}]\!]}{[\![\sigma_{ij}]\!]}\left(\varepsilon_{ij}^{e}\bar{E}_{ijkl}\varepsilon_{ij}^{e}-\frac{1}{9}\left(\frac{1}{1+cY^{+}\exp(-dY^{+})}\right)(\varepsilon_{mm}^{e})^{2}\delta_{ij}\bar{E}_{ijkl}\delta_{kl}\right) \tag{25}$$

$$Y^{-}=\frac{1}{2}\frac{[\![\sigma_{ij}^{-}]\!]}{[\![\sigma_{ij}]\!]}\left(\varepsilon_{ij}^{e}\bar{E}_{ijkl}\varepsilon_{ij}^{e}-\frac{1}{9}\left(\frac{1}{1+cY^{-}\exp(-dY^{-})}\right)(\varepsilon_{mm}^{e})^{2}\delta_{ij}\bar{E}_{ijkl}\delta_{kl}\right) \tag{26}$$

In the above equation, c and d indicate the constants of the materials. These equations have also been used for modeling the elastic-plastic-damage of concrete [18]. Damage conjugate forces presented in Eq. (25) and (26) were calculated by differentiating from the elastic part of the free energy. Using these equations in the elastic-damage model will not lead to any problems, while it is necessary to take into account the plasticity effect on the conjugate forces for models that consider the plasticity effects [14, 19]. Therefore, in this study, Eq. (27) and (28) which include the plasticity effects were used for calculation of the conjugate forces [19].

$$Y^{+}=\frac{1}{2}\frac{[\![\sigma_{ij}^{+}]\!]}{[\![\sigma_{ij}]\!]}\left(\varepsilon_{ij}^{e}\bar{E}_{ijkl}\varepsilon_{ij}^{e}\right)+f_{0}^{+}\kappa^{+}+\frac{1}{2}h(\kappa^{+})^{2} \tag{27}$$

$$Y^{-}=\frac{1}{2}\frac{[\![\sigma_{ij}^{-}]\!]}{[\![\sigma_{ij}]\!]}\left(\varepsilon_{ij}^{e}\bar{E}_{ijkl}\varepsilon_{ij}^{e}\right)+f_{0}^{-}\kappa^{-}+Q\left(\kappa^{-}+\frac{1}{w}exp(-w\kappa^{-})\right) \tag{28}$$

Eq. (23) is investigated in each computational step {damage variables of the previous step are considered in Eq. (24)}. If the value of $g^{\pm}$ is less than or equal to zero, no change will be applied on the damage variable; otherwise, the values of the damage variables, assuming $g^{\pm}=0$, will be calculated using Eq. (29). Subsequently, the numerical variable of damage will be calculated using Eq. (6).

$$\varphi^{\pm}=1-\frac{1}{1+\left(a^{\pm}\left[Y^{\pm}-Y_{0}^{\pm}\right]\right)^{b^{\pm}}} \tag{29}$$

Using the isotropic damage in this model causes the damage to affect the biaxial response of the problem. This effect can be eliminated by modification of a^{-} [18]. Voyiadjis and Taqieddin [18] have presented an equation for modification of a^{-} based on biaxial strains. This relation, in a more general case, can be shown as follows:

$$a^{-}=a_{0}^{-}\left(1-\gamma\left[\left(\frac{\langle-\varepsilon_{22}\rangle}{\langle-\varepsilon_{11}\rangle}\right)^{\frac{1}{12}}+\left(\frac{\langle-\varepsilon_{33}\rangle}{\langle-\varepsilon_{11}\rangle}\right)^{\frac{1}{12}}\right]\right) \tag{30}$$

In Eq. (30), a_{0}^{-} indicates the value resulted from the uniaxial loading or the initial value of this constant. Further, ε_{11}, ε_{22}, and ε_{33} are the main strains. This equation is dependent on the direction. The main direction is the direction that has less negative strain and is identifiable under the name of ε_{11} in implementation of the model. In Eq. (30), γ is a coefficient calculated through trial and error with compressive strength of at least one biaxial compressive state. It should be noted that in case of uniaxial loading, Eq. (30) has no

effect on a^-.

In addition to the constants which are calculable based on the mechanical properties of materials, the proposed model includes 9 constants of Q, w, h, $Y_0^{\pm}$, $a^{\pm}$, and $b^{\pm}$ which have no clear experimental definition. In this study, the genetic algorithm optimization method was used to calculate these constants. Regarding the equations in the model of Voyiadjis and Taqieddin [18], it can be easily understood that in modeling the uniaxial tension, only the constants of h ،Y_0^+ ،a^+, and b^+ affect the results; furthermore, in uniaxial compression modeling, only the constants of Q ،w ، Y_0^- ،a^-, and b^-will be effective [18]. As a result, in this research, the constants of the proposed model are determined separately based on uniaxial tensile and compressive tests. Here, the values of α and Poisson's ratio were considered 0.121 and 0.2, respectively, similarly to the literature [14, 15, 18].

3. IDENTIFICATION OF CONSTANTS USING GENETIC ALGORITHM

3.1. Genetic algorithm

Genetic Algorithm (GA) is a member of the family of computational methods based on artificial intelligence [23]. This method imitates the biological evolution process that leads to the survival of the fittest genes or individuals [24]. GA has been widely used for searching the optimal values of responses for multi-dimensional problems with several parameters. In using this method for multivariable problems, each value of the variables is a chromosome, and each response that is a set of chromosomes is called an individual. Each response in this method is a set of values of variables that satisfies all the bounds [24]. GA starts from a set of initial responses (first generation). Then, the competency of each individual is evaluated using the objective function. To achieve the optimal response, the individuals should be changed and generate new individuals. Genetic Algorithm uses three main operators including *selection*, *combination*, and *mutation*, inspired from the natural evolution, to produce generations and improve responses. The *selection* operator used in this study serves to choose the parents based on the previous generation with regard to the competency level of the individuals. Using the *combination* operator in a random process between two parents leads to the production of a child with a combination of the parents' characteristics. *Mutation* is a very important operator in the genetic algorithm. Because, by exerting random changes on the parents for production of children, it prevents the produced children's entrapment in the local minimums. Therefore, the whole response space is investigated. The mutation rate must be considered low, because a high rate of mutation destroys the competency of better individuals [25]. Fig. 2 shows the optimization process by GA. In this study, GA tools in MATLAB were utilized [26].

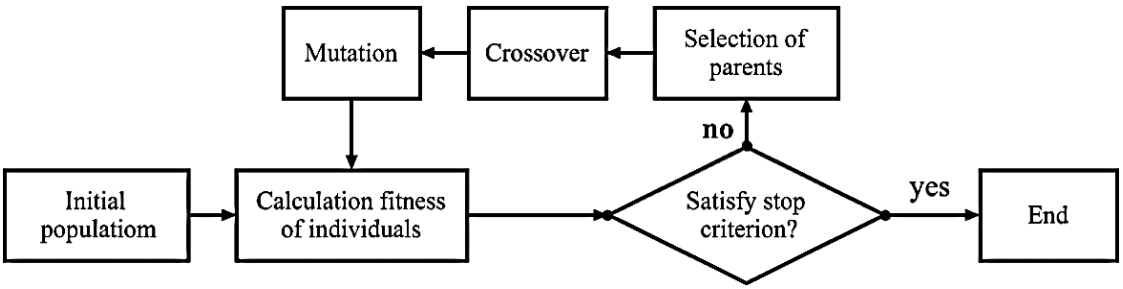

Figure 2. Simple flowchart of genetic algorithm performance

3.2 Objective function

In this study, the objective function was determined based on the rate of consistency between the experimental results and the results of modeling the compressive and tensile uniaxial stress-strain diagram. Similarly to studies by Wardeh and Toutanji [22], the objective function ($F_{objective}$) is calculated as a function of the stress resulted from the modeling, and the stress resulted from experimental results at a point with constant strain {Eq. (31)}.

$$F_{objective} = f(\sigma(\varepsilon_i, calculation), \sigma(\varepsilon_i, experimental)) \tag{31}$$

To reduce the effect of high-error points on the overall result, the sum of absolute errors was considered as the form of the function f {Eq. (32)} instead of using the sum of error squares function. By minimizing this function, GA achieves the optimal value for the constants of the problem.

$$F_{objective} = \frac{1}{n}\sum_{i=1}^{n}\left|\frac{\sigma(\varepsilon_i, calculation) - \sigma(\varepsilon_i, experimental)}{\sigma(\varepsilon_i, experimental)}\right| \tag{32}$$

In the above equation, n is the number the points tested for compliance, and ε_i is the strain in i^{th} step in the step-by-step modeling.

To achieve the optimal values of constants of the Voyiadjis and Taqieddin's model [18], this model was implemented in MATLAB for an element under the uniaxial loading with regard to the presented objective function. To optimize the model constants, the GA tool of this software was used [23]. The code written in MATLAB software environment had the capability to execute, for each set of the proposed GA constants, the uniaxial loading modeling function for compression or tension, and report the value of the objective function to GA based on the obtained stress-strain diagram. It should be noted that in addition to the points required to determine the objective function, a number of midpoints were also used for determining the responses in order to achieve more accurate responses by shrinkage of the loading steps. The values of the probability ratio of mutation and combination operators were 30% and 70%, respectively, in this research. Due to high computational cost of each time of code execution, the initial population was considered as including 50 chromosomes and the GA process continued until achieving the optimal values of up to 100 generations. In the genetic algorithm method, a domain can be considered for the constants, because proper

and limited selection of this domain helps improving the accuracy of the problem. In this research, the appropriate values of the constants domain were determined in some of the samples following an initial optimization without considering a value for the domain. Investigation of several samples made it possible to easily predict these domains with regard to the experimental diagram, especially for the damage constants. Moreover, the accuracy of the domains was examined based on the final response. If the final response was close to the boundaries assigned to the constants, then the optimization process would be re-conducted with increase of the response domain.

3.3 Optimization of plasticity and damage tensile constants based on uniaxial tensile test

In the uniaxial tension state, it is assumed that plasticity and damage are initiated exactly at the outset of the softening response [16-18]. Accordingly, Y_0^+ can be directly calculated by calculating the equivalent strain tensor (ε_{ij}^{et}) in the maximum uniaxial tensile strength when the hardening variable is zero (κ^+), and placing these values in Eq. (27) {Eq. (33)}.

$$Y_0^+ = \frac{1}{2}\frac{[\![\sigma_{ij}^+]\!]}{[\![\sigma_{ij}]\!]}\left(\varepsilon_{ij}^{et}\bar{E}_{ijkl}\varepsilon_{ij}^{et}\right) \tag{33}$$

Results of 14 experimental samples of the uniaxial tensile tests collected from the relevant literature were used in this section (Table 1) [27-36]. For each sample, mechanical properties required for modeling were determined based on the experimental results (Table 1). Then, the damage and plasticity constants of each sample were optimized using GA. Table 1 presents these results together with the values of the objective function of the most optimal mode.

To examine the accuracy of the results, the uniaxial tensile test diagrams resulted from the modeling and experimental results were compared with each other in Fig. 3. For a better demonstration of the results, samples with high ultimate strains were shown separately {Fig. 3(a)}. As seen in this figure, there is an appropriate agreement between the experimental and modeling results.

Table 1: Mechanical properties and results of GA for uniaxial tensile

Specimen	Mechanical properties			GA results				
	E (MPa)	f_c (MPa)	f_t (MPa)	Y_0^+	h	b^+	a^+	$F_{objective}$
T1 (Meng et al. [27])	16400	37.1	2.03	0.000126	13127	1.210	2400	0.132
T2 (Meng et al. [27])	24522	67.6	3.70	0.000279	3877	1.126	1920	0.093
T3 (Meng et al. [27])	38318	83.0	4.60	0.000276	2964	1.416	941	0.169
T4 (Huo et al. [28])	45493	46.8	4.49	0.000221	4404	0.849	6254	0.152
T5 (Reinhardt et al. [29])	30288	47.1	3.44	0.000195	3643	1.178	975	0.089
T6 (Reinhardt et al. [29])	16576	48.6	2.56	0.000198	3214	1.455	1177	0.086
T7 (Yan and Lin [30])	28265	65.0	2.22	0.000087	4181	1.205	8661	0.072
T8 (Akita et al. [31])	39370	33.4	2.88	0.000105	3536	1.006	5403	0.127
T9 (Akita et al. [31])	38291	29.7	3.25	0.000138	8573	1.043	1714	0.074
T10 (Gopalaratnam and	31000	46.8	3.53	0.000201	1136	1.096	5705	0.088

Shah [32])								
T11 (Zhang [33])	34403	47.2	3.40	0.000168	3175	1.848	8258	0.083
T12 (Li et al. [34])	20347	46.8	4.01	0.000394	4969	1.116	950	0.073
T13 (Ren et al. [35])	35999	65.0	2.59	0.000093	4015	0.999	2335	0.090
T14 (Kupfer et al. [36])	30072	32.1	2.91	0.000135	3669	1.018	19379	0.042

3.4 Optimization of plasticity and damage compressive constants based on uniaxial compressive test

Results of 30 experimental samples of uniaxial compression collected from the relevant literature were used in this section (Table 2) [35-44]. For each sample, mechanical properties required for modeling were determined based on the experimental results (Table 2).

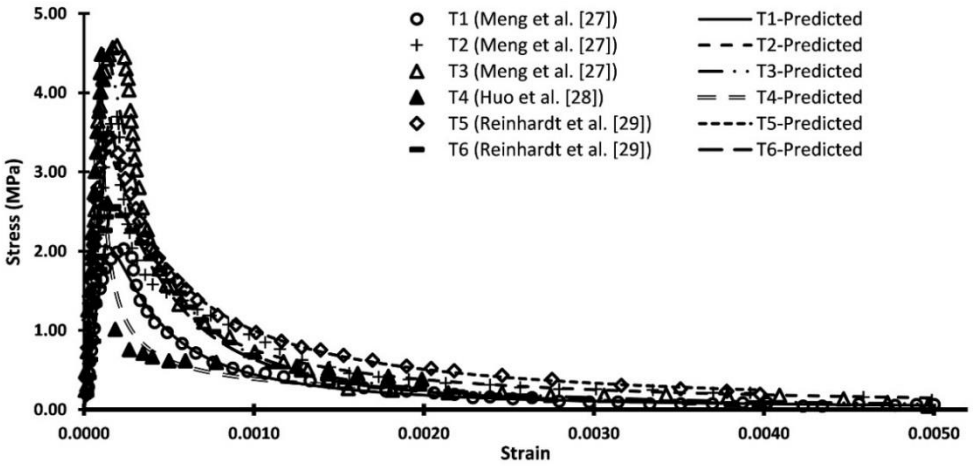

(a) T1-T6

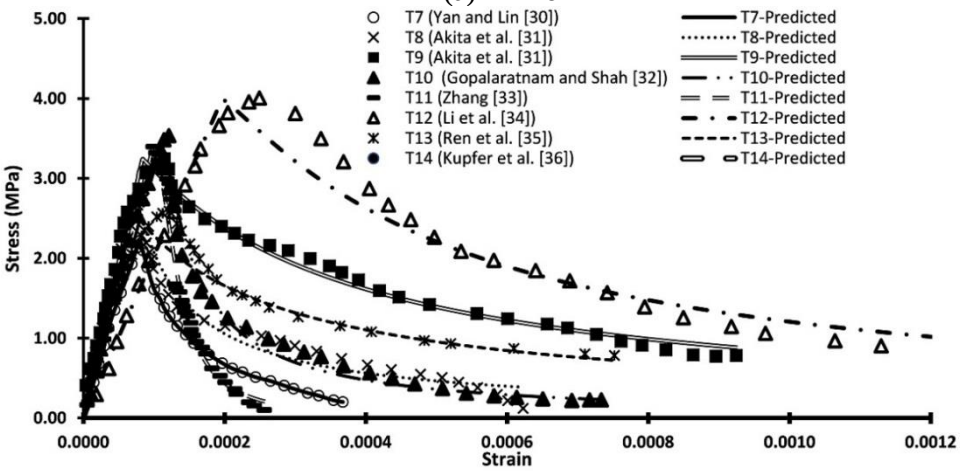

(b) T7-T14

Figure 3. Comparison of stress-strain diagrams of uniaxial tensile test obtained from modeling and experimental results

The equivalent elasticity modulus of each test was calculated, with respect to the proposed regulations of ACI-318 [45], based on the uniaxial compressive stress-strain

diagram: the front-line slope from the coordinates origin to a point with tension of 0.45 fc was considered as equal to the elasticity modulus. f_0 is a stress after which the nonlinear response is initiated in the uniaxial compressive stress-strain diagram [18]; in other words, decrease of the diagram slope begins in this stress. This value was determined by investigating the changes in the slope of the experimental uniaxial compressive stress-strain diagram. In optimization of the compressive constants, Y_0^- was introduced to GA as an unspecified constant. But in several sequential execution of the genetic algorithm for a particular sample, different values were calculated for the compressive constants and some instability was observed in the GA responses. To solve this problem, as in the uniaxial tension state, it was assumed that plasticity and damage are initiated simultaneously. In another study, Wu et al. [16] considered initiation of damage to be shortly before plasticity; thus, this assumption is not unachievable. Based on Equation 28, when the hardening variable of (κ^-) is 0, Y_0^-can be calculated by placing the equivalent strain tensor of (ε_{ij}^{ec}) in the uniaxial compressive stress of the outset of the nonlinear response (f_0) {Eq. (34)}. As it can be observed, Eq. (34) is dependent on the Q/w ratio. Therefore, this equation was presented in form of a code in the software so that a new Y_0^- is calculated for each individual in each execution of GA.

$$Y_0^- = \frac{1}{2}\frac{[\![\sigma_{ij}^-]\!]}{[\![\sigma_{ij}]\!]}\left(\varepsilon_{ij}^{ec}\bar{E}_{ijkl}\varepsilon_{ij}^{ec}\right) + \frac{Q}{w} \tag{34}$$

Table 2: Mechanical properties and results of GA for uniaxial compressive test

Specimen	Mechanical properties			GA results					
	E (MPa)	f_0 (MPa)	f_c (MPa)	Y_0^-	W	Q	b^-	a^-	$F_{objectiv}$
C1 (Wee et al. [37])	49051	58.7	122.6	0.2065	756.2	129.6	6.968	5.22	0.051
C2 (Wee et al. [37])	45658	58.0	105.7	0.1871	687.6	103.4	2.249	4.33	0.068
C3 (Wee et al. [37])	42871	50.6	85.8	0.1426	725.8	81.8	2.009	6.00	0.063
C4 (Wee et al. [37])	41070	23.7	66.6	0.0700	1261.5	79.6	1.967	6.01	0.050
C5 (Wee et al. [37])	36463	29.4	46.7	0.0556	867.0	37.9	1.580	9.94	0.062
C6 (Wee et al. [37])	28412	16.3	30.9	0.0365	881.5	28.0	1.314	13.39	0.041
C7 (Li and Ren [38])	38808	15.2	51.2	0.0395	1940.8	70.8	2.126	9.47	0.016
C8 (Karsan and Jirsa [39])	31000	10.9	27.6	0.0233	1365.8	29.3	1.109	18.11	0.025
C9 (Ali et al. [40])	13820	10.0	16.7	0.0174	763.4	10.5	1.783	29.72	0.031
C10 (Ali et al. [40])	19980	12.7	25.3	0.0261	968.9	21.4	1.790	18.58	0.057
C11 (Ali et al. [40])	23530	9.0	27.7	0.0161	1997.7	28.7	1.452	14.75	0.016
C12 (Ali et al. [40])	33980	9.1	32.0	0.0198	1901.5	35.3	1.039	15.04	0.016
C13 (Ali et al. [40])	44550	10.0	43.5	0.0281	1956.6	52.7	1.056	10.26	0.042
C14 (Kupfer [36])	30072	13.2	32.1	0.0322	975.0	28.6	1.307	13.58	0.029
C15 (Dahl [41])	18050	9.7	22.0	0.0244	820.9	17.9	1.072	16.67	0.017
C16 (Dahl [41])	25493	10.2	32.1	0.0375	883.4	31.3	1.367	11.23	0.040
C17 (Dahl [41])	33574	11.0	50.1	0.0550	1127.1	59.9	2.050	7.39	0.050
C18 (Dahl [41])	33990	18.0	65.0	0.0757	1109.5	78.6	2.769	6.96	0.071
C19 (Dahl [41])	40595	39.2	93.5	0.1365	880.5	103.5	5.513	6.29	0.056
C20 (Dahl [41])	41361	84.2	105.4	0.5218	175.4	76.5	3.903	9.46	0.057
C21 (Carreira and Chu [42])	27177	36.5	46.4	0.1418	238.0	27.9	2.144	10.98	0.027
C22 (Carreira and Chu [42])	23115	22.0	34.9	0.0559	557.9	25.3	1.906	12.17	0.029
C23 (Carreira and Chu [42])	18748	7.9	20.0	0.0076	3044.5	18.1	1.166	21.68	0.026
C24 (Carreira and Chu [42])	26033	23.8	73.6	0.1283	698.4	82.0	4.088	4.47	0.031

C25 (Carreira and Chu [42])	20974	19.5	50.7	0.0643	1070.4	59.1	2.697	7.14	0.036
C26 (Carreira and Chu [42])	17222	17.4	40.5	0.0522	965.5	42.0	2.419	8.97	0.039
C27 (Carreira and Chu [42])	10636	6.7	20.7	0.0103	2290.8	18.7	1.674	13.92	0.020
C28 (Muguruma and Watanabe [43])	38105	33.3	65.6	0.1907	387.0	68.1	0.909	3.83	0.045
C29 (Sinha et al. [44])	20197	9.6	26.0	0.0289	957.5	25.5	1.296	12.82	0.028
C30 (Ren et al. [35])	39772	41.0	65.0	0.1040	682.1	56.6	1.907	9.97	0.091

After calculating the mechanical properties, damage and plasticity constants and, subsequently, the value of Y_0^- were optimized for each sample using GA. Table 2 shows these results together with the values of the objective function of the most optimal state. By comparing the values of objective functions of the compressive and tensile samples, a higher precision is observed for the compressive state (Tables 1 and 2). This can be due to the higher capacity of the model proposed by Voyiadjis and Taqieddin [18] in modeling the uniaxial compressive tests. The uniaxial compressive test diagrams of the samples in two categories with compressive resistance of higher and lower than 50 MPa were compared with the results of modeling in Fig. 4 and 5, respectively. In these figures, a good agreement is observable between experimental and modeling results. This agreement indicates the appropriate optimization of the damage and plasticity constants. Further, despite the reduction in the accuracy of modeling for the concrete with very high compressive resistance, it can be said that the model presented by Voyiadjis and Taqieddin [18] can efficiently model concrete in a wide range of compressive resistance (see Fig. 4 and 5).

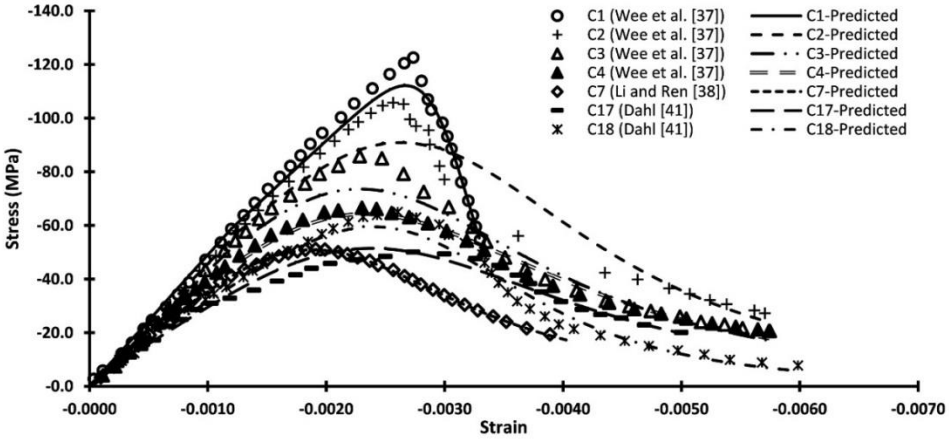

(a) Part I

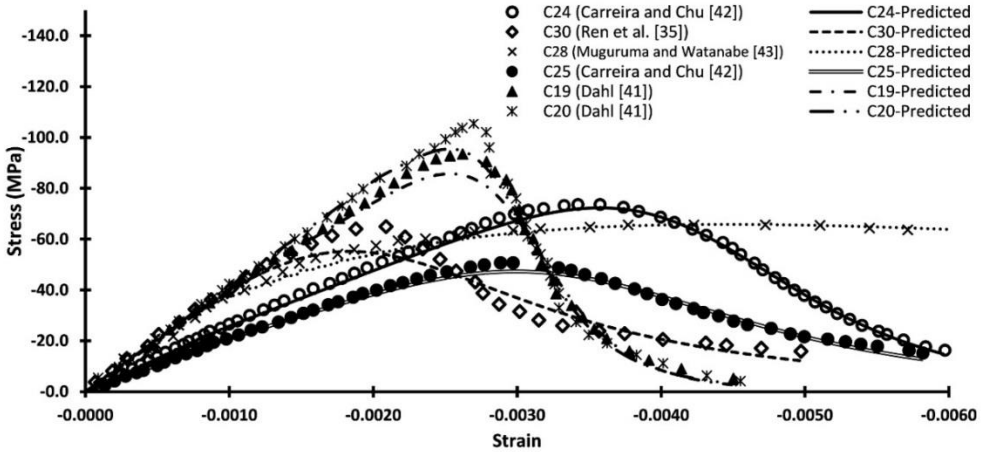

(b) Part II

Figure 4. Comparison of stress-strain diagrams of uniaxial compressive tests obtained from experimental and modeling results of samples with compressive resistance of more than 50 MPa

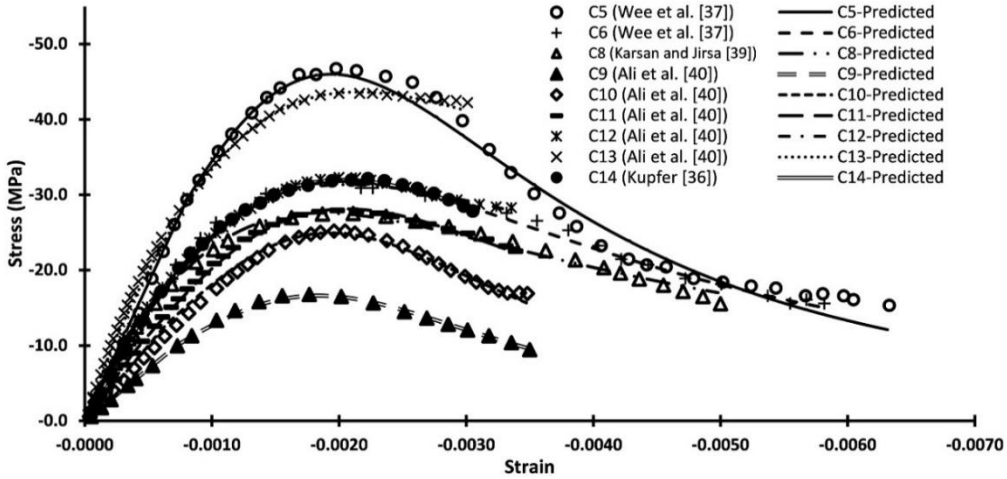

(a) Part I

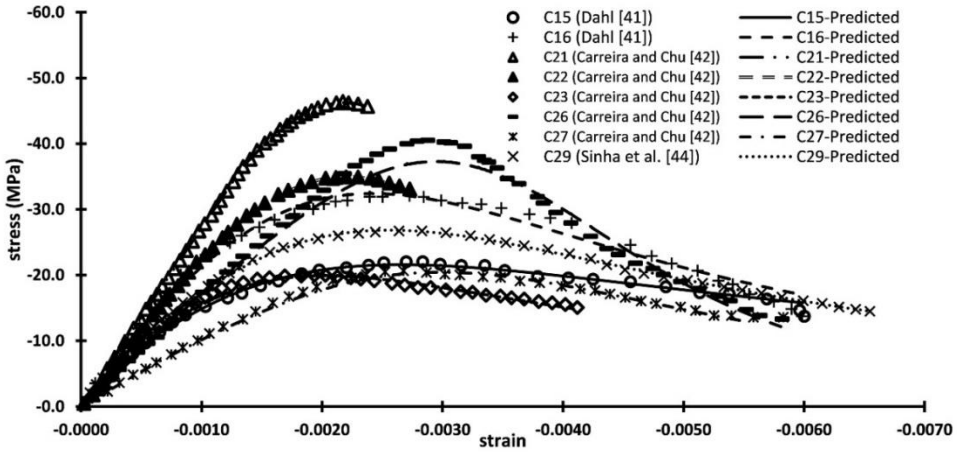

(b) Part II

Figure 5. Comparison of stress-strain diagrams of uniaxial compressive tests obtained from

experimental and modeling results of samples with compressive resistance of less than 50 MPa

4. COMPARISON OF MODELING RESULTS IN UNIAXIAL COMPRESSIVE AND TENSILE TESTS WITH OTHER STUDIES

In Fig. 6, the results of modeling the uniaxial compressive and tensile tests obtained from this research have been compared with those of two other valid studies conducted in this field. The stress-strain diagram of specimens C8 and T11 in all three studies were predicted with similar accuracy (Fig. 6); however, a better modeling has been accomplished for sample T10 in the present study {Fig. 6(b)}.

4.1 Investigation of GA optimization results

- ***Cyclic tests***

For applying more control on the GA results, six cyclic compressive and tensile tests taken from the relevant literature were investigated in this section [29, 32, 39, 43, 44]. In the cyclic tests, the irreversible strains are clearly visible. Success in predicting the results is an evidence of appropriate modeling of the materials plasticity.

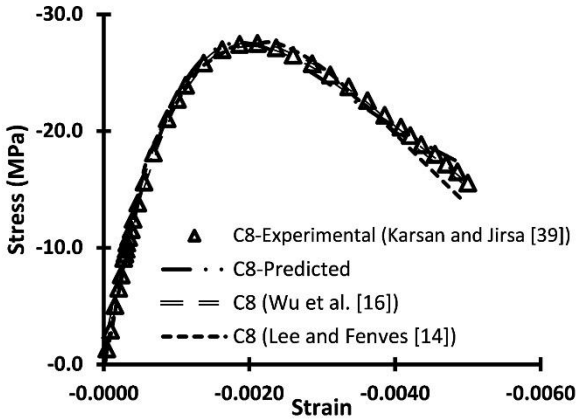

(a) uniaxial compressive stress-strain diagram

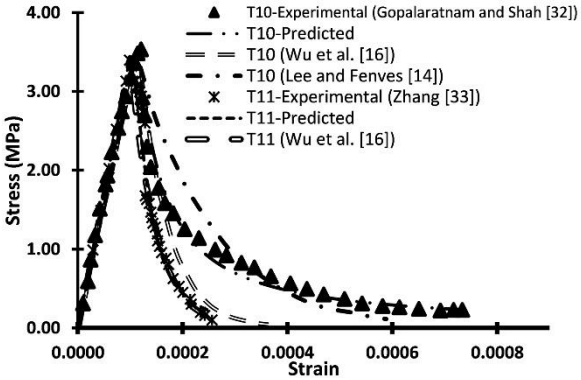

(b) uniaxial tensile stress-strain diagram

Figure 6. Comparison of results of modeling the uniaxial compressive and tensile tests with

other studies strain diagram

- **Cyclic tensile test**

Fig. 7 shows the experimental results of cyclic tension for samples TC5, TC6, and TC10, corresponding to the uniaxial tensile samples T5, T6, and T10 [29, 32]. This test was simulated in MATLAB environment and the results presented in Table 1 were used for the damage and plasticity constants of each sample. The modeling results were compared with the experimental results in Fig. 7. There was an appropriate consistency between the corresponding diagrams. In Fig. 7(b), results of modeling sample TC10 were also compared with the modeling results of two other valid references. Fig. 7(b) shows superiority of the results of the present study.

- **Cyclic compressive test**

Samples CC8, CC28, and CC29 were made of materials similar to that of samples C8, C28, and C29, and were investigated using cyclic compressive tests [39, 43, 44], To model these samples, the GA results were used for their corresponding uniaxial compressive samples. Fig. 8 shows the experimental and modeling results for the introduced samples. In higher strains, there is a little difference between the experimental and modeling results. The author's investigations showed that this difference was due to the nature of the used plastic model and could also be seen in modeling results presented in the relevant literature [14-16].

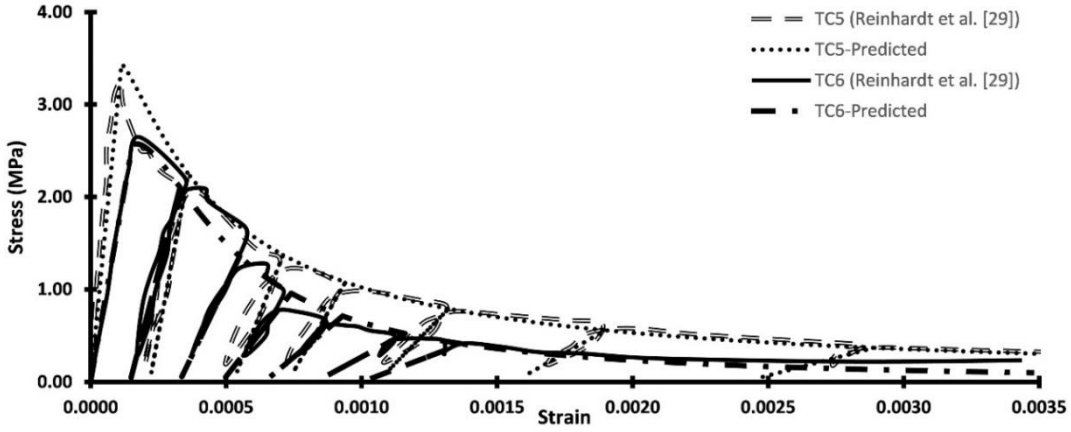

(a) TC5 and TC6

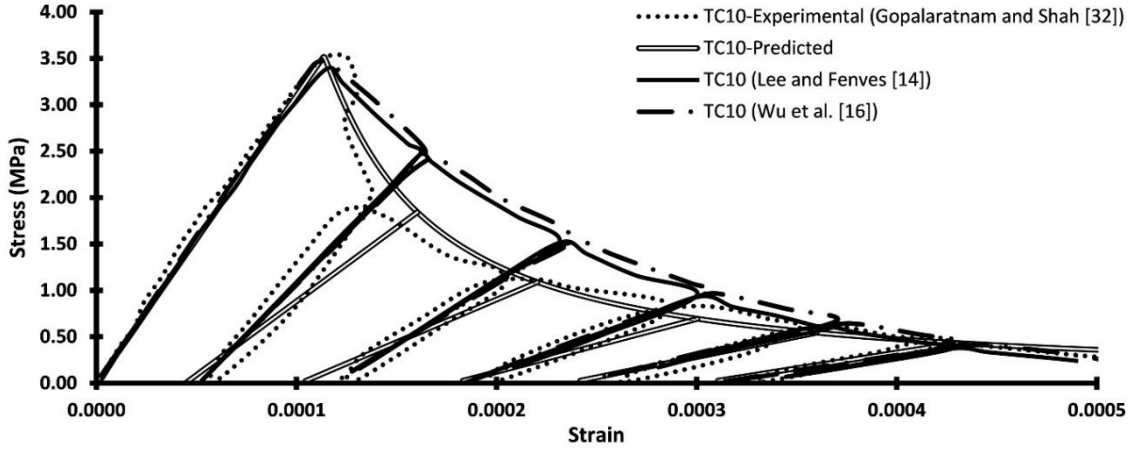

(b) TC10

Figure 7. Comparison of stress-strain diagrams of cyclic tensile tests obtained from experimental and modeling

In Fig. 8(b), the results of modeling sample CC8 were compared with the results of modeling in two other references. In this figure, although a better response has been presented by Lee and Fenves [14] and Wu et al. [16], it should be noted that the damage and plasticity constants in these studies have been obtained inversely and by matching the results. Yet, in the present study, these constants have been calculated only based on the results of uniaxial tensile and compressive tests.

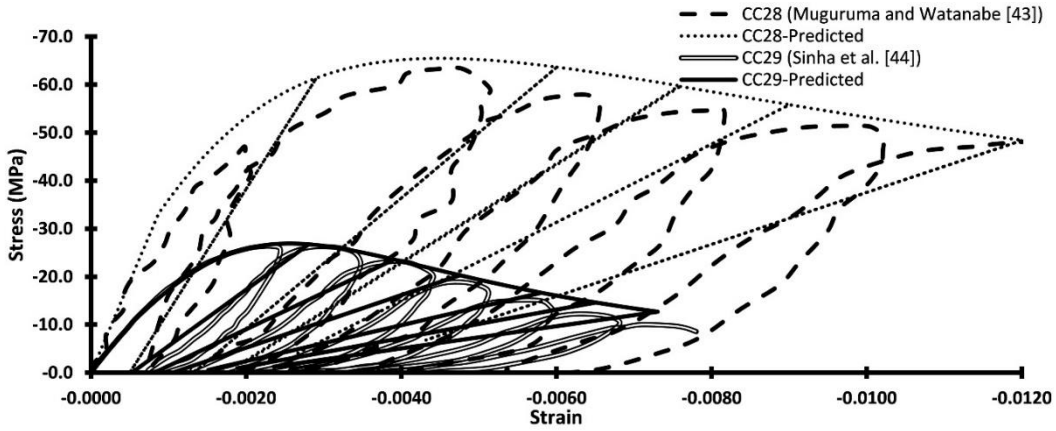

(a) CC28 and CC29

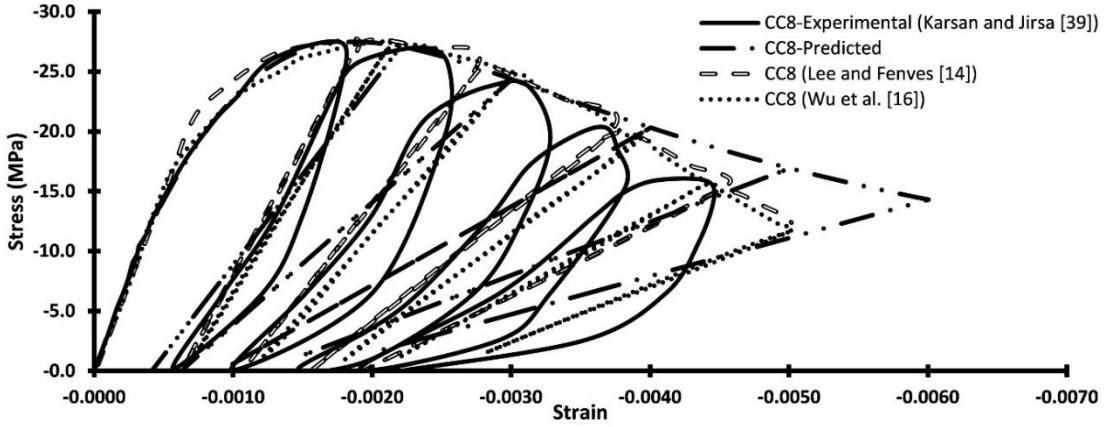

(b) CC8

Figure 8. Comparison of stress-strain diagrams of cyclic compressive tests obtained from experimental and modeling

- **Biaxial tests**

In this section, the performance of model presented in Section (2) and the accuracy of proposed GA coefficients for modeling biaxial compressive test as well as the biaxial failure envelope for samples concrete of C14 and C7 will be investigated. Conducting the biaxial compressive test requires the determination of γ coefficient. This coefficient can be calculated using GA, based on the value of the ultimate resistance of at least one bi-axial compressive test and modeling it when other damage and plasticity constants remain unchanged. For this purpose, the difference between the modeling and experimental ultimate strength in the biaxial state can be presented as the objective function. The values of these coefficients for the biaxial samples corresponding to C7 and C14 were calculated as 0.538 and 0.421, respectively. In Fig. 9(a), the stress-strain diagram of the biaxial compressive test with different applied strain ratios for the concrete corresponding to sample C7 was compared with the results of modeling based on the constants provided in Table 2. In this figure, the diagrams resulted from the stress-strain modeling were in good agreement with the experimental results; however, their ultimate strength was correctly predicted. The concrete biaxial test which contains a descending branch is one of the most complex tests. Further investigations are required to justify the reason of difference between the experimental and modeling results, which was not possible in this research due to the limited experimental results in this field. This error may be due to different experimental and modeling conditions, or even an experimental error.

One of the most important diagrams obtained from the biaxial tests is the failure envelope. The failure envelope diagram corresponding to the concrete used in samples T14 and C14 is presented in Fig. 9(b) based on the results of Kupfer et al. [36]. Using the results of samples T14 and C14 as well as the value of γ calculated in the previous section, the biaxial failure envelope diagram of this concrete is illustrated in Fig. 9(b) and compared with the corresponding experimental results. In this diagram, there is a good agreement between modeling and experimental results; moreover, the modeling response presented in this section is slightly conservative compared to other studies. This type of response is desirable in the field of civil engineering {Fig. 9(b)}.

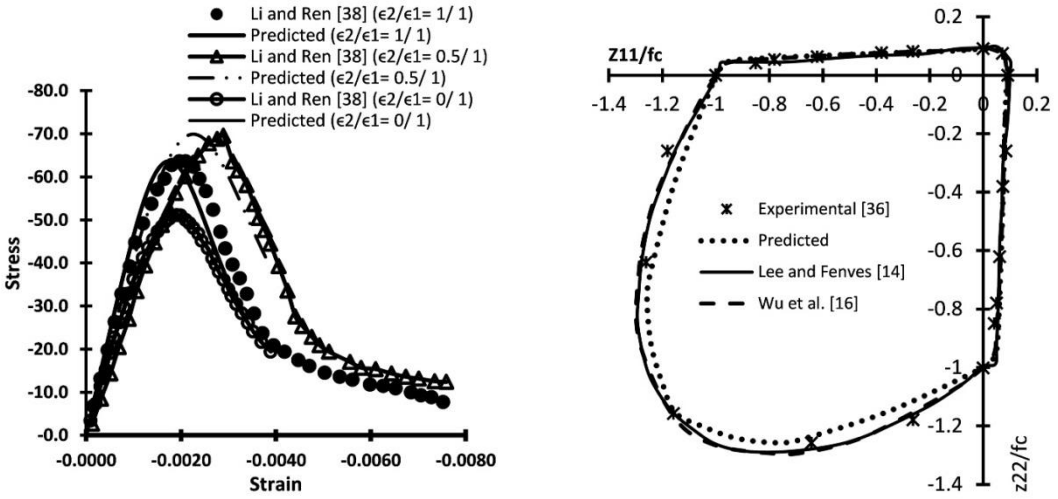

(a) Stress-strain diagram of biaxial compressive test for the concrete corresponding to specimens C7

(b) Failure envelope for concrete corresponding to specimens T14 and C14

Figure 9. Comparison of experimental and modeling results, biaxial tests

5. SUMMARY AND CONCLUSION

In the present study, in order to determine the constants of an elastic-damage-plastic model proposed for concrete, the results of 44 uniaxial compressive and tensile tests were used. These constants were determined for all the samples using the GA optimization tool by investigating the consistency of experimental and modeling results. Then, the resulted constants were investigated for modeling a number of tests representing the behavioral nature of concrete.

The results of this study are summarized as follows:

- GA could accurately determine the constants of damage and plasticity based on the uniaxial tests. Investigation of the GA results for modeling the uniaxial, biaxial, and cyclic tests indicated the accuracy of these values for constitutive modeling of concrete.
- According to the investigations conducted in this study, the quotation proposed in the relevant literature stating that "determination of the constants of damage and plasticity through comparison of modeling and experimental results of the uniaxial compressive and tensile tests", seems to be an appropriate suggestion. Nevertheless, using the trial and error method might lead to elimination of the plasticity response of the problem.
- The model used in this study demonstrated its ability to cover a wide range of concrete resistance; nonetheless, this model is less consistent with the uniaxial tension diagram than with the uniaxial compressive diagram.

REFERENCES

1. Aïtcin PC. Cements of yesterday and today: concrete of tomorrow, *Cement Concre Res* 2000; **30**(9): 1349-59.
2. Gencel O. Physical and mechanical properties of concrete containing hematite as aggregates, *Sci Eng Compos Mater* 2011; **18**(3): 191-9.
3. Chaboche JL. Continuous damage mechanics-a tool to describe phenomena before crack initiation, *Nuclear Eng Des* 1981; **64**(2): 233-47.
4. Buyukozturk O, Shareef SS. Constitutive modeling of concrete in finite element analysis, *Comput Struct* 1985; **21**(3): 581-610.
5. Bangash M. Concrete and concrete structures: Numerical modelling and applications, 1989.
6. Chen WF, Saleeb AF. Constitutive equations for engineering materials, elasticity and modeling, *Stud Appl Mech* 1994; **37**: 1-580.
7. Béton Ce-id. RC *Elements Under Cyclic Loading: State of the Art Report*: Thomas Telford, 1996.
8. Dilmaç H, Demir F. Stress–strain modeling of high-strength concrete by the adaptive network-based fuzzy inference system (ANFIS) approach, *Neural Comput Applicat* 2013; **23**(1): 385-90.
9. Sahin U, Bedirhanoglu I. A fuzzy model approach to stress–strain relationship of concrete in compression, *Arabian J Sci Eng* 2014; **39**(6): 4515-27.
10. Samani AK, Attard MM. A stress–strain model for uniaxial and confined concrete under compression, *Eng Struct* 2012; **41**: 335-49.
11. Lu ZH, Zhao YG. Empirical stress-strain model for unconfined high-strength concrete under uniaxial compression, *J Mater Civil Eng* 2010; **22**(11): 1181-6.
12. Babu R, Benipal G, Singh A. Constitutive modelling of concrete: an overview, *Asian J Civil Eng (Building and Housing)* 2005; **6**: 211-46.
13. Tao X, Phillips DV. A simplified isotropic damage model for concrete under bi-axial stress states, *Cement Concr Compos* 2005; **27**(6): 716-26.
14. Lee J, Fenves GL. Plastic-damage model for cyclic loading of concrete structures, *J Eng Mech* 1998; **124**(8): 892-900.
15. Jason L, Huerta A, Pijaudier-Cabot G, Ghavamian S. An elastic plastic damage formulation for concrete: Application to elementary tests and comparison with an isotropic damage model, *Comput Method Appl Mech Eng* 2006; **195**(52): 7077-92.
16. Wu JY, Li J, Faria R. An energy release rate-based plastic-damage model for concrete, *Int J Sol Struct* 2006; **43**(3): 583-612.
17. Al-Rub RKA, Voyiadjis GZ. Gradient-enhanced coupled plasticity-anisotropic damage model for concrete fracture: computational aspects and applications, *Int J Dam Mech* 2008.
18. Voyiadjis GZ, Taqieddin ZN. Elastic plastic and damage model for concrete materials: Part I-Theoretical formulation, *Int J Struct Chang Sol* 2009; **1**(1): 31-59.
19. Taqieddin ZN, Voyiadjis GZ, Almasri AH. Formulation and verification of a concrete model with strong coupling between isotropic damage and elastoplasticity and comparison to a weak coupling model, *J Eng Mech* 2011; **138**(5): 530-41.

20. Liu J, Lin G, Zhong H. An elastoplastic damage constitutive model for concrete, *China Ocean Eng* 2013; **27**: 169-82.
21. Oliveira S, Toader A-M, Vieira P. Damage identification in a concrete dam by fitting measured modal parameters, *Nonline Analy: Real World Applicat* 2012; **13**(6):2888-99.
22. Wardeh MA, Toutanji HA. Parameter estimation of an anisotropic damage model for concrete using genetic algorithms, *Int J Damage Mech* 2015:1056789515622803.
23. Chipperfield A, Fleming P, editors. The MATLAB genetic algorithm toolbox, Applied control techniques using MATLAB, IEE Colloquium on IET, 1995.
24. Goldberg DE, John H. Holland. Genetic algorithms and machine learning, *Mach Learn* 1988; **3**(2-3): 95-9.
25. Eiben AE, Smith JE. Introduction to evolutionary computing: Springer; 2003.
26. Naderpour H, Kheyroddin AA, Arab-Naeini M. Cost optimum design of prestressed concrete bridge decks based on bridge loading iranian code using genetic algorithm, *Transport Eng* 2015; **6**(2): 355-69.
27. Meng Y, Chengkui H, Jizhong W. Characteristics of stress-strain curve of high strength steel fiber reinforced concrete under uniaxial tension, *J Wuhan University Technol Mater Sci Edit* 2006; **21**(3): 132-7.
28. Huo HY, Cao CJ, Sun L, Song LS, Xing T, editors. Experimental study on full stress-strain curve of SFRC in axial tension, *Appl Mech Mater* 2012; **238**: 41-5.
29. Reinhardt HW, Cornelissen HA, Hordijk DA. Tensile tests and failure analysis of concrete, *J Struct Eng* 1986; **112**(11): 2462-77.
30. Yan D, Lin G. Experimental study on concrete under dynamic tensile loading, *J Civil Eng Res Pract* 2006; **3**(1): 1-8.
31. Akita H, Koide H, Tomon M. Uniaxial tensile test of unnotched specimens under correcting flexure, AEDIFICATIO Publishers, Fracture Mechanics of Concrete Structures, 1998; **1**: 367-75.
32. Gopalaratnam V, Shah SP, editors. Softening response of plain concrete in direct tension, *Aci Mater J* 1985; **82**(3): 310-23.
33. Zhang Q. Research on the stochastic damage constitutive of concrete material: Ph. D. Dissertation, Tongji University, Shanghai, China, 2001.
34. Li Z, Kulkarni S, Shah S. New test method for obtaining softening response of unnotched concrete specimen under uniaxial tension, *Experiment Mech* 1993; **33**(3): 181-8.
35. Ren X, Yang W, Zhou Y, Li J. Behavior of high-performance concrete under uniaxial and biaxial loading, *ACI Mater J* 2008; **105**(6): 548-57.
36. Kupfer H, Hilsdorf HK, Rusch H, editors. Behavior of concrete under biaxial stresses, *J Eng Mech Div* 1973, 99(4): 853-66.
37. Wee T, Chin M, Mansur M. Stress-strain relationship of high-strength concrete in compression, *J Mater Civil Eng* 1996; **8**(2): 70-6.
38. Li J, Ren X. Stochastic damage model for concrete based on energy equivalent strain, *Int J Sol Struct* 2009; **46**(11): 2407-19.
39. Karsan ID, Jirsa JO. Behavior of concrete under compressive loadings, *J Struct Div* 1969; **95**(12): 2543-64.
40. Ali AM, Farid B, Al-Janabi A. Stress-Strain Relationship for concrete in compression made of local materials, *Eng Sci* 1990; **2**(1) 183-94.

41. Dahl KK. Uniaxial stress-strain curves for normal and high strength concrete: Afdelingen for Baerende Konstruktioner, Danmarks Tekniske Højskole, 1992.
42. Carreira DJ, Chu KH, editors. Stress-strain relationship for plain concrete in compression, *J American Concr Institute* 1985; **82**(6): 797-804.
43. Muguruma H, Watanabe F, editors. Ductility improvement of high-strength concrete columns with lateral confinement, *Proceedings of the Second International Symposium on Utilization of High-Strength Concrete*, 1990.
44. Sinha B, Gerstle KH, Tulin LG. Stress-strain relations for concrete under cyclic loading, *J American Concr Institute* 1964; **61**(2): 195-211.
45. Committee A, Institute AC, Standardization IOf, editors. Building code requirements for structural concrete (ACI 318-08) and commentary 2008, American Concrete Institute.